Development and Application of Discontinuous Modelling for Rock Engineering, Ming Lu (ed.) 2003 Swets & Zeitlinger, Lisse. pp: 93 – 102.

Deformation and kinematics of vertically jointed rock layers in underground openings

M. Tsesarsky and Y. H. Hatzor
Department of Geological and Environmental Sciences. Ben Gurion University of the Negev. P.O.B 653. Beer-Sheva 84105, Israel.

ABSTRACT: Layered and jointed rock masses are common in underground environments. Honest stability analysis of such rock masses requires the application of discrete element methods, since other methods of analysis are either continuous by nature (FEM), or limited to two block interaction (Voussoir model). In this paper the stability of jointed rock layers is studied using DDA. Two different configurations are studied: 1) single layer-immediate roof; 2) multi-layered roof. The influence of joint spacing and shear strength is investigated and different failure modes are discussed; the kinematics and evolution of deformation are studied in depth. For a single layer configuration it is shown that stable arching is achieved when the shear resistance along joints is sufficient to inhibit inter-block shear and to induce block rotation at the abutments. For a multi-layered configuration it is found that the transition from unstable multi-layer deflection due to vertical load transfer, to stable arching is marked by reduction of differential deflections and homogenization of displacement within the stack of layers. The numeric solution is compared with the semi-analytical Voussoir solution, which for the given rock mass structure and mechanical properties, is found to be un-conservative.

1 INTRODUCTION

All rock masses contain discontinuities, such as joints, beddings, and faults. Discontinuities are sources of weakness in an otherwise competent rock mass. At shallow depth where stresses are low, failure of intact rock is minimal and the behavior of the rock mass is controlled by sliding on discontinuities.

A stratified rock mass, a succession of parallel layers whose thickness is small compared with the span of the opening, is a common feature in mining and civil engineering where excavation in sedimentary rock is attempted. If an opening is excavated in this type of rock, the roof of the excavation will part from the rock mass due to the low tensile strength of bedding planes, thus forming the immediate roof. Fayol (1885) demonstrated that within a stack of simply supported beams the gravitational load of the upper beams was transmitted laterally to the supports rather than vertically to the lower members. For such a configuration beam theory can be employed to assess deflection, shear stresses, and maximum stresses in the immediate roof (e.g. Obert and Duvall, 1967; Goodman 1989).

In practice, stratified rock masses are in most cases transected by numerous joints forming a matrix of individual rock blocks. The analysis of a stratified and jointed roof is complicated by the fact that there is no closed-formed analytical solution for the interaction of these blocks. Evans (1941) established the relationship between vertical deflection, lateral thrust and stability of a jointed beam, with a single crack at mid-span and two abutment joints - the*"Voussoir Beam"* analogy (Figure 1). Beer and Meek (1982) reformulated and extended Evans's approach and introduced a coherent system of static equations, Brady and Brown (1985) introduced an iterative algorithm for the evaluation of voussoir beam stability. Further improvements of the method were introduced by Sofianos (1996), and Diederichs and Kaiser (1999).

The major advantages of the voussoir beam technique are the ability to assess previously ignored failure mode of shear along the abutments, and the static (although undetermined) formulation of the discussed problem. Two main disadvantages of this method are: 1) the geometrical and mechanical properties of the transverse joints are overlooked; and 2) only a single layer of the roof is considered. It is reasonable to assume that the mutual interaction of the individual blocks and the layers in laminated and stratified rock masses will differ from those described by Fayol. In the absence of an analytical solution, the stability of underground openings in laminated and jointed rock masses should be sought by means of numerical analysis.

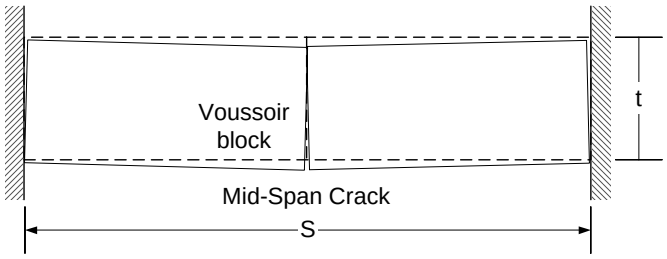

Figure 1. The Voussoir model of a discontinuous beam.

Wright (1972) compared two models of voussoir beams using linear FEM, from single mid-span joint to multi jointed and concluded that the voussoir with a single mid-span joint is the worst case. Passaris et al., (1993) have shown that crushing in high stresses area and shear sliding are the most common failure modes encountered in mining environments, and showed that Wright's conclusion was erroneous. In their study however, the crushing failure was studied under pre-conditioning of no shear along the joints. Ran et al., (1994) studied the behavior of a jointed beam using non-linear FEM, and showed that the no shear pre-conditioning may result in overly conservative estimate of roof strength. Both Passaris et al., and Ran et al., extended their analysis to multiple joints of variable spacing, however friction along joints was not modeled. FEM have limited applicability to the analysis of jointed rock masses since only small displacements/rotations are allowed, full detachment between elements is not allowed, and new contacts are not automatically detected. Furthermore, a large number of joint elements in the FEM analysis may lead to ill-conditioning and numerical instabilities (Jing and Hudson, 2002).

Sofianos and Kapenis (1998) studied the stability of the classic mid-span jointed voussoir beam using UDEC (Cundall, 1971; Itasca 1993), using however unrealistic joint properties: $\phi = 0^0$ at mid span, and $\phi = 89^0$ and cohesion $c = 10GPa$ at the abutments. Thus, elastic displacement at mid-span is prevented, and only separation without shear is allowed at the abutments, i.e. crushing will occur before slip commences. Nomikos et al., (2002) modeled the structural response of a multi-jointed roof rock beams, using UDEC, under similar assumptions. Young (1991) studied the stability of a synthetic roof mine using DDA. Hatzor and Benari (1998) used DDA in back analysis of historic roof collapse in an underground water storage system, showing the influence of joint spacing and friction on the overall stability of multi-jointed roof.

In the present paper, we explore the kinematics of single and multi- layered fractured rock beams using DDA. The analysis addresses both mechanical and geometrical properties of the transverse joints without preconditioning using realistic rock mass properties. The failure of the ancient water reservoir of Tel Beer-Sheva is revisited using newly attained data regarding beam geometry, joint mechanical properties and mechanical properties of intact rock. The results of DDA and classic Voussoir are compared.

2 DISCONTINUOUS DEFORMATION ANALYSIS (DDA)

DDA (Shi 1989, 1993) is the implicit member of the Discrete Element Method group. DDA models a discontinuous material as a system of individually deformable blocks that move independently without interpenetration. In the DDA method the formulation of the blocks is very similar to the definition of a finite element mesh. A finite element type of problem is solved in which all elements are physically isolated blocks bounded by pre-existing discontinuities. The blocks used in DDA can assume any given geometry, as opposed to the predetermined topologies of the FEM elements.

In DDA individual blocks form a system of blocks through contacts among blocks and displacement constrains on individual blocks. For a block system defined by n blocks the simultaneous equilibrium equations are $\mathbf{KD} = \mathbf{F}$ where $\mathbf{K}$ is the global stiffness matrix, $\mathbf{D}$ is the displacement variables vector and $\mathbf{F}$ is the forcing vector. The total number of displacement unknowns is the sum of degrees of freedom of all blocks. The simultaneous equations are derived by minimizing the total potential energy Π of the block system. A complete description of stiffness matrix and load vector assembly is found in Shi (1993).

The solution of the system of simultaneous equilibrium equations is constrained by inequalities associated with block kinematics: no penetration and no tension condition between blocks. The kinematic constrains on the system are imposed using the penalty method. Shear displacement along the interfaces is modeled using Coulomb - Mohr failure criterion. The solution of the system of equations is iterative. First, the solution is checked to see how well the kinematical constrains are satisfied. If tension or penetration are found along contacts the constrains are adjusted by selecting new positions for the contact springs and modified versions of $\mathbf{K}$ and $\mathbf{F}$ are formed for which a new solution is attained. The process is repeated until each of the contacts converges to a constant state. The positions of the blocks are then updated according to the prescribed displacement variables. The large displacements and deformations are the accumulation of small displacements and deformations at each time step.

The accuracy of DDA has been tested by many researchers. Yeung (1991), MacLaughlin (1997) and Doolin and Sitar (2002) studied the accuracy of DDA for slope stability analysis under gravitational loadings. Hatzor and Feintuch (2001) validated DDA using direct dynamic input. O'sullivan and

Development and Application of Discontinuous Modelling for Rock Engineering, Ming Lu (ed.) 2003 Swets & Zeitlinger, Lisse. pp: 93 – 102.

Bray (2001) simulated the behavior of hexagonally packed glass rods subjected to bi-axial compression, showing the advantages of DDA in the study of soil dynamics. McBride and Scheele (2001) validated DDA using a multi-block array on stepped base subjected to gravitational loading, and a bearing capacity model. Tsesarsky et al., (2002) compared between shaking table and DDA results.

Successful validation of numerical models by closed form solutions for simple problems, or by comparison to small-scale physical models is essential. However, no analytical solution or laboratory model can duplicate the scale and character of the loading, boundary and environmental conditions inherent to full-scale problems. Comparison of numerical predictions to actual behavior in well-documented case studies can help insure that the extrapolation from simple problems to field scale problems is basically valid.

3 THE TEL BEER-SHEVA CASE STUDY

3.1 *Geometrical and geological setting*

The ancient site of Tel Beer-Sheva (2700 B.P to 3200 B.P) is located approximately 3 km South – East of the modern city of Beer Sheva. Situated on a hilltop (+307 m.s.l.), the site is bordered by two ephemeral streams. The ancient water reservoir beneath the site is dated to 3000 B.P. The large storage facility was fed by seasonal run-offs, through a tunnel running beneath the city walls. The intake capacity of the reservoir was approximately 250 m^3. The walls of the reservoir were plastered to prevent leakage. The excavation sequence of the water reservoir is unknown. However, evidence of failure within the period of excavation, or short time after, are found in the form of a large support pillars coated with the same plaster. The water reservoir layout is presented in Figure 2. Two pillars, found at the center of the reservoir, support the roof at areas where failure occurred.

The water reservoir was excavated in the sedimentary Gareb formation (Upper Cretaceous), comprised of alteration of horizontal layers of chalk 0.3m to 0.8m thick, with some thinner (up to 0.1m) layers of low plasticity and low swelling potential marl (Benary, 1996). The overall thickness of chalk beds above the excavation roof is 5m.

3.2 *Rock mass structure*

The rock mass structure consists of three vertical joint sets and a horizontal bedding plane (Benary, 1996). The geometrical properties of the joint sets are given in Table 1. Joint sets J1 and J2 are most abundant with mean spacing of 0.2m and 0.25m respectively. The bedding planes are horizontal with mean spacing of 0.5m. The strike of joint set J1 is nearly parallel to the axis of the intake tunnel, while J2 is perpendicular to J1 and co-linear with the reservoir walls. The intersections of the closely spaced joints (J1 and J2) with the bedding planes form a dense network of mostly equidimensional cubic blocks. J3 is less abundant and in most cases is not a part of a block forming joint combination.

Table 1. Discontinuity data for the Tel Beer-Sheva rock mass, from Benary (1996). SV – sub vertical, V – vertical, H – horizontal.

Set #	Dip	Strike ^{o}	Spacing m	Persistance m
1	SV	039-061	0.2	>10
2	SV	125-127	0.25	Bounded by #1
3	V	107-112	1.6	> 15
Bedding	H		0.5	Infinite

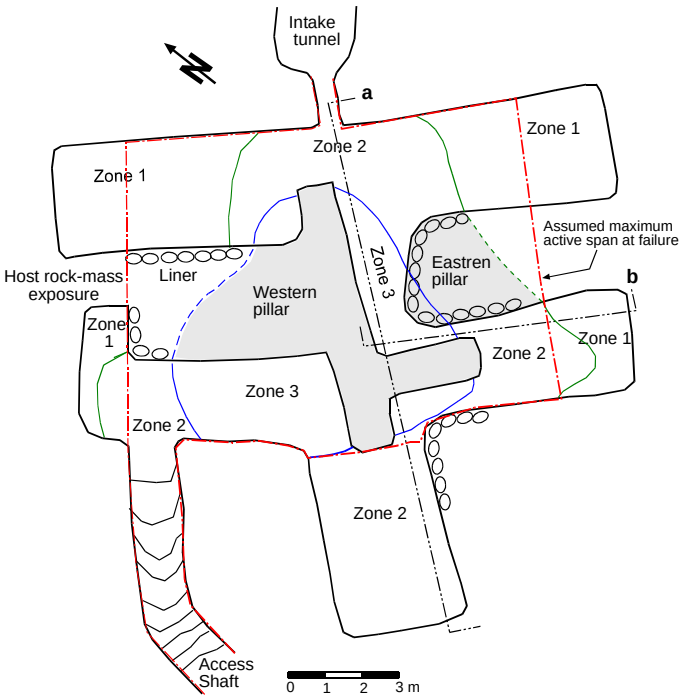

Figure 2. Layout of the Tel Beer-Sheva water reservoir and the morphology of the failure zones, modified after Benary (1996).

3.3 *Failure zone morphology*

The roof of the water reservoir collapsed into a shape of a three dimensional dome. Three distinct levels were mapped by Benary (1996), refer to Figure 2: 1) Original excavation level at +286 m.s.l – Zone 1; 2) Intermediate failure level at +287 m.s.l – Zone 2; 3) Upper failure level at +289 m.s.l – Zone 3. All zones are developed along natural bedding planes. The transition between the different levels is ranging from vertical to step like, running along block boundaries.

The western pillar supports the roof at Zone 3. The lateral extent of the pillar is unknown due to plaster coating. However, given the fact that the pillar supports the uppermost failure zone, the minimum extent is within the boundaries of Zone 3. The Eastern pillar supports Zone 2, and does not attain

Zone 3.Based on these observations the assumed minimum active span of the opening at the time of failure was 8 meters, conforming to Zone 3. The assumed maximum active span was 10, meters conforming to Zone 2.

3.4 *Strength and elasticity of intact rock*

Intact rock samples (NX size cylinders) were tested using hydraulic, close-loop, servo-controlled, triaxial load frame with stiffness of 5×10^9 N/m (TerraTek system model FX-S-33090). All tests were performed under a constant strain rate of 10^{-5} s^{-1}. The cylinder axes were oriented parallel to bedding planes (the angle between the normal to bedding planes and maximum principal stress σ_1 is $\beta = 90^o$). The Uniaxial Compressive Strength (UCS) in the parallel to bedding direction is 28 MPa, whereas at normal to bedding ($\beta = 0^\circ$) UCS = 7 MPa (Benari, 1996). Gareb chalks exhibit pronounced anisotropy both in strength and in elasticity. The unixial compressive strength ratio ($UCS_{\beta=90^o}/UCS_{\beta=0^o}$), and the elastic modulus ratio ($E_{\beta=90^o}/E_{\beta=0^o}$) are both about 4. The mechanical properties of the Gareb chalk are summarized in Table 2.

Table 2. Mechanical properties of the Gareb chalk. β is the angle between the normal to bedding to maximum principal stress, ρ is density, n is porosity, E is the elastic modulus, ν is poisons ration and UCS is uniaxial compressive strength. * data from Benary (1996).

β (^{o})	ρ 10^3kg/m^3	n %	E MPa	ν	UCS MPa
90	1.9	29	7840	0.17	28
0*	1.91	29	1900	0.005	7

3.5 *Shear strength of discontinuities*

The mechanical properties of the discontinuities were tested using hydraulic, close-loop, servo-controlled, direct shear system (manufactured by TerraTek) with normal force capacity of 1000 kN and horizontal load capacity of 300 kN. The stiffness of the normal and shear load frames were 7.0 MN/m and 3.5 MN/m respectively. Joint displacement was monitored by 6 LVDTs, 4 for normal displacement and 2 for shear displacement, all of which had 50 mm range and 0.25% linearity full scale. The shear box size is capable of accepting samples of size up to 150 mm × 150 mm × 300mm.

Direst shear test were performed on both natural joint and polished surfaces. The joint was tested as sampled without any additional treatment. The results are presented in Figure 3a, and the variation of resulting friction angle as a function of normal stress is given in Figure 3b. Peak friction angle under the specified loading condition was $\phi_p = 47^o$, the friction angle was reduced during the test down to a value of $\phi_r = 24^o$. Direct shear of polished surfaces yielded similar value for residual friction angle: $\phi_r = 25^o$.

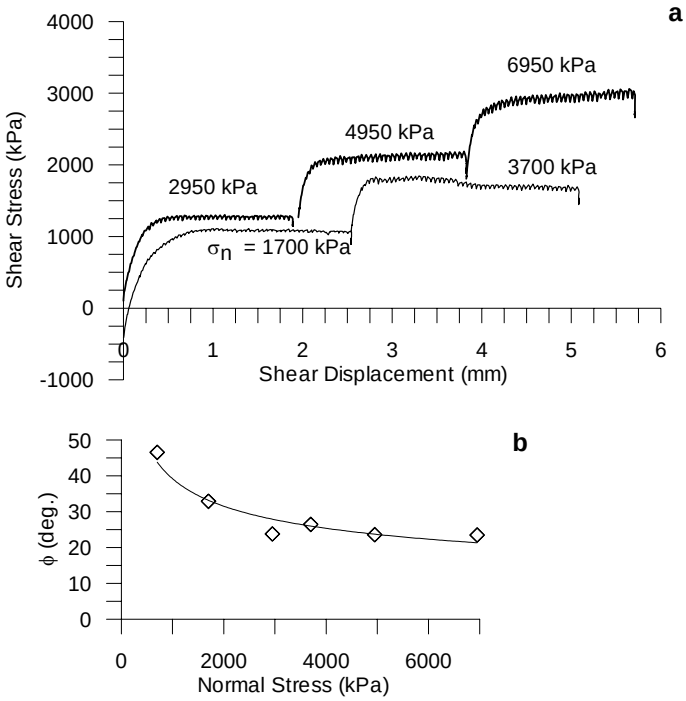

Figure 3. a) Shear Stress – Shear displacement curves for natural joint sample TBS-1; b) Friction angle degradation as function of normal stress.

4 STABILITY ANALYSIS OF TEL BEER-SHEVA WATER RESERVOIR – THE VOUSSOIR ANALOGUE

Stability analysis of the Tel Beer-Sheva water reservoir was performed using the iterative procedure introduced by Brady and Brown (1985). Since the rock mass was found to be transversely isotropic the values of E, ν, and UCS chosen for the analysis were the values measured in the direction parallel to bedding, which is horizontal for the case of a roof in horizontally layered roof.

The factor of safety against failure in compression and shear was calculated for a wide range of beam geometries. The beam span (S) was varied from 5m to 16m, and beam thickness (t) was varied from 0.25m to 5m, thus accounting for most likely geometries at time of failure. The factor of safety ($F.S.$) against failure in compression as a function of beam thickness is plotted in Figure 4a. For beam thickness lower than 0.5 m and span greater than 10m the predicted failure mode is by snap trough (buckling). The factor of safety against failure in compression for all other geometries is greater than 3, increasing with beam thickness due to larger moment arm (Z) and lower axial stress (f_c).

The factor of safety against shear along abutments for friction angles ranging from $\phi = 20^\circ$ to $\phi = 70^\circ$ is plotted in Figure 4b, where the beam span is normalized to beam thickness. Assuming that the peak friction angle along joints is $\phi = 47^\circ$ and that

Development and Application of Discontinuous Modelling for Rock Engineering, Ming Lu (ed.) 2003 Swets & Zeitlinger, Lisse. pp: 93 – 102.

the active span at time of failure was 8m, the factor of safety against shear is ranging from $F.S. = 8.3$ to $F.S. = 0.83$ for beam thickness ranging from 0.5m to 5m respectively.

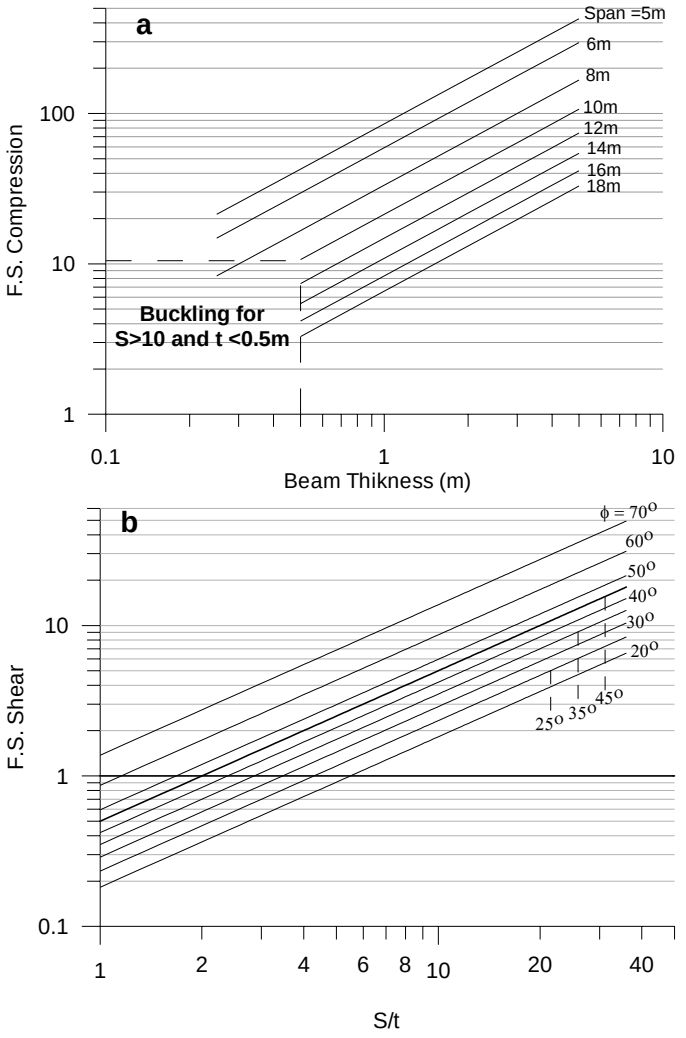

Figure 4. Factors of safety again failure for the Tel Beer-Sheva ware reservoir: a) failure in compression; b) shear along abutments.

Assuming a roof span of 8m and layer thickness of 5m the failure of the ancient water reservoir at Tel Beer Sheva can be explained using the Voussoir analysis. However, this is not the case, the thickness of Zone 3 is 1m to 2m which is the maximum active thickness of the failed layer. Given a thickness of 2m the factor of safety against shear failure is $F.S. = 2$, for beam thickness of 1m the factor of safety is even higher than $F.S. > 4$. For active span greater than 8m the factor of safety rises above 1 for all thickness values considered. Moreover, for beam with $r = S/t > 4$, the required friction angle for stability is $\phi > 25^{\circ}$. Therefore, under the given geometrical constrains and material properties the Beer and Meek procedure predicts stable roof, in contrast to field evidence.

5 DDA ANALYSIS OF THE TEL BEER-SHEVA WATER RESERVOIR

DDA analysis of the Tel Beer-Sheva ancient water reservoir was performed for two geometric configurations: 1) a single layer of thickness *t = 0.5 m*, representing the immediate roof of the excavation, Figure 5a; and 2) a sequence of layers, each of thickness *t = 0.5 m*, attaining a total thickness of 5m, conforming to the actual chalk thickness, Figure 5b. The active span of both modeled configurations was set to *S =8m*. While configuration 1 is compatible with the Voussoir model, configuration 2 is a realistic model of the chalk layers comprising the rock mass at the water reservoir. Two fixed blocks, each containing three fixed points, represent the abutments.

Material properties and numeric control parameters of DDA analysis are given in Table 3. The joints are modeled as no-tension, no-cohesion interfaces, with purely frictional shear resistance, in compliance with field findings.

Table 3. Numeric control parameters of DDA analysis

E	7840 MPa
ν	0.17
ρ	
Time step size	0.00025 sec
Penalty stiffness	1000 MN/m
Penetration control parameter	0.00025
Dynamic control Parameter	1

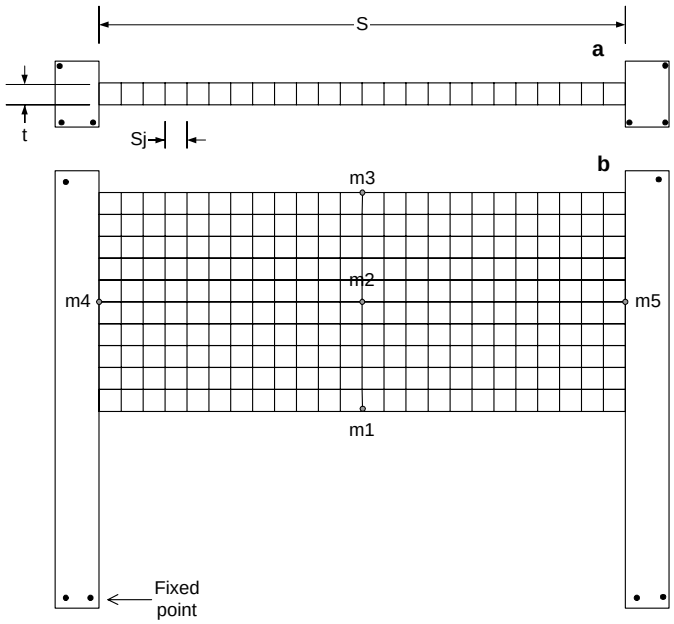

Figure 5. Geometry of the DDA analysis: a) single layer; b) stack of layers.

The effect of joint friction was studied for a constant joint spacing of $S_j = 0.25m$ (in accordance with the average spacing of J1, J2) while the friction along joints (ϕ_{av}) was varied from $\phi_{av} = 20^{o}$ to $\phi_{av} = 80^{o}$. The effect of joint spacing was studied for $\phi_{av} = 47^{o}$ (ϕ_p from direct shear tests) while joint spacing was changed from $S_j = 0.25m$ to $S_j = 4m$. For con-

figuration 1 the displacements where measured at the lower fiber of the beam at selected points in intervals of *0.5m*. For configuration 2 the displacements where measured at five locations: 1) *m1 (x_0, y_0)*- mid-span of immediate roof; 2) *m2 (x_0, y_0+2.5m)*; 3) *m3 (x_0, y_0+5m)*; 4) *m4 (x_0+4m, y_0+2.5m)*; *5) m5 (x_0-4m, y_0+2.5m)*.

5.1 *DDA analysis of a single multi-jointed layer*

The results of DDA analysis for the single layer configuration are presented in Figure 6a, which is a plot of mid-span deflection (δ) after *0.25sec* versus friction angle (ϕ) and joint spacing (S_j). Figures 6b and 6c are time histories of mid-span deflection for different values of friction angle and joint spacing respectively. DDA graphic outputs of single beam deformation for selected values of friction angle are given in Figure 7.

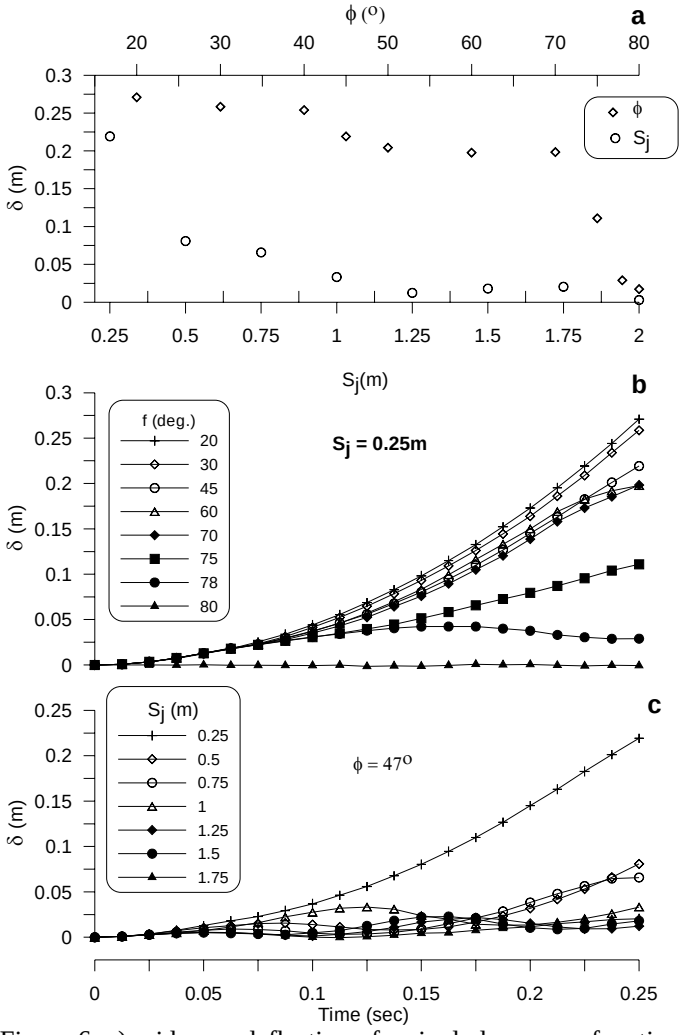

Figure 6. a) mid-span deflection of a single layer as a function of joint spacing (S_j) and friction (ϕ); b) mid-span deflection time histories for selected values of friction for S_j = *0.25m*; c) and friction (ϕ); b) mid-span deflection time histories for selected values of joint spacing (S_j), for $\phi = 47^o$.

Given joint spacing of S_j = *0.25m* the beam progressively deflects, and eventually fails, for friction angles of $\phi_{av} < 78^o$. For friction angles of $\phi_{av} \geq 78^o$ the beam attains stable equilibrium after small initial deflection. Figures 8a, b, and c show the displacements, *u, v,* and the rotation ω respectively, of the beam lower fiber after *0.25sec* for selected values of friction angle: a) 30^o; b) 45^o; c) 75^o; d) 80^o.

At low values of $\phi_{av} = 30^o$ and $\phi_{av} = 45^o$ most of the deformation is achieved through deferential inter-block shear, which attains maximum at the mid-span and minimum at the abutments. The rotation of the blocks is mostly uniform and symmetric, up to ±0.1 radians, where at the left hand side of the beam the blocks rotate clockwise and vice versa. A similar beam deflection profile was attained by Evans (1941) while experimenting with brick beams. The deformation characteristics are changed when the friction angle along the joints rises above $\phi_{av} = 75^o$; inter-block shear is reduced while the rotation at the beam ends rises to ±0.3 radians.

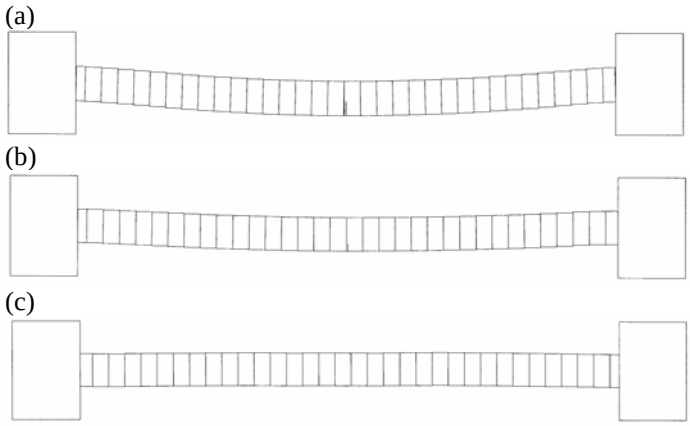

Figure 7. DDA graphic outputs of single layer deformation for *S = 8m*, S_j = *0.25m* and *t = 0.5m* at *T = 0.25 sec*: a) $\phi = 47^o$; b) $\phi = 75^o$; c) $\phi = 80^o$.

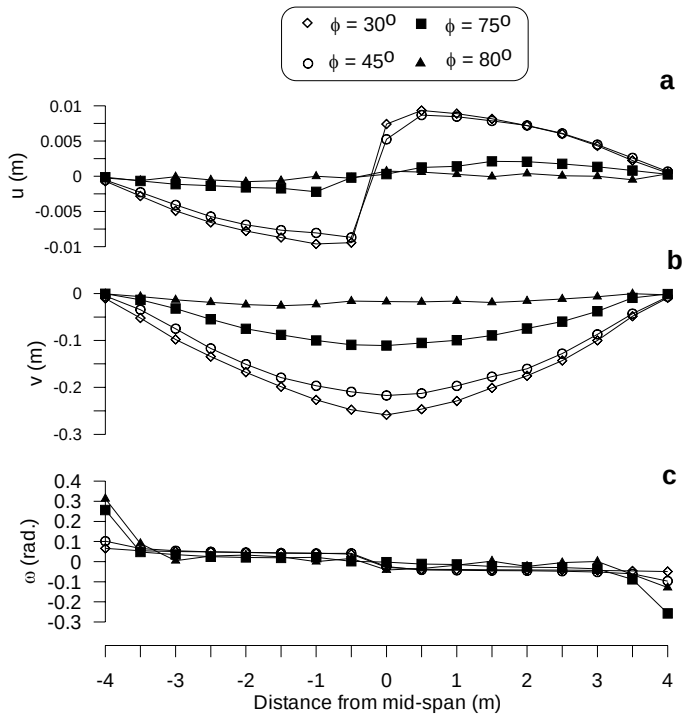

Figure 8. DDA deformation variables for a single layer model, measured at the lowermost fiber of the beam: a) horizontal displacement (u); b) vertical displacement (v); and c) rotation (ω).

From the rotation data, it is evident that at low values of friction angle the moment arm of the lateral couple does not developed effectively and beam

Development and Application of Discontinuous Modelling for Rock Engineering, Ming Lu (ed.) 2003 Swets & Zeitlinger, Lisse. pp: 93 – 102.

deformation occurs mainly due to inter-block shear, which consequently leads to failure. Where the available shear resistance along joints is sufficiently high to preclude excessive vertical displacements, block rotation and build-up of lateral thrust equilibrate the overturning moment of the vertical couple, and the beam reaches equilibrium position.

Increasing the block dimension ratio ($r_b = S_j/t$) of the individual blocks by setting $S_j = 0.5m$ ($r_b = 1$), and assuming peak friction angle of $\phi_{av} = 47^o$ (peak friction angle from direct shear), results in mid-span deflection of $\delta = 0.08\,m$ (after *0.25 sec)*, compared with $\delta = 0.22\,m$ for $S_j = 0.25m$. However, the beam does not attain equilibrium, and eventually fails. Examination of the deformation time histories for beams of different aspect ratios (Figure 6c) reveals that equilibrium is marked by the oscillatory nature of the solution, as opposed to gradually increasing deflection of failing beams. Equilibrium is met when $r_b \geq 2.5$ ($S_j \geq 1.25$) and $\delta \leq 0.025\,m$. The style of deformation is similar: for unstable geometry the beam fails by inter-block shear, with relatively small rotations, while for stable geometries stability is achieved trough effective rotation.

The underlying assumption of immediate roof (single layer) analysis is that vertical load from overlaying layers is transmitted laterally to the abutments, rather than vertically as transverse loads to the lower layers. This condition is not satisfied within the layers overlying the water reservoir, namely the failure zone is up to 2.5m thick. Given average bed thickness of $t = 0.5m$ the failure zone contained 5 individual layers. The stability of a multi-layered and jointed structure, the laminated Voussoir beam (a term introduced by Hatzor and Benary, 1998), is explored in the following section.

5.2 *DDA analysis of a sequence of multi-jointed layers*

The results of DDA analysis for the laminated Voussoir configuration are presented in Figure 9a, which is a plot of mid-span deflection (δ) after 0.25sec versus friction angle (ϕ) and joint spacing (S_j). The deflection data is given at measurement points *m1, m2* and *m3.* Time histories of the three measurement points for different values of joint spacing are presented in Figure 9b,c,d. DDA graphic outputs of multi-layered roof deformation for selected values of friction angle are given in Figure 10.

For block dimension ratio of $r_b = 0.5$ the deflections are excessive for all friction angle values analyzed, and failure is expected. Furthermore, the deflections trough the stack of layers shows that $\delta_{m1} > \delta_{m2} > \delta_{m3}$, suggesting that each layer is vertically loaded by overlying layers. The lowermost layer bears most of the vertical load and consequently deflection attains maximum value, decreasing with vertical distance from the immediate roof. For $\phi_{av} < 50^o$ the deflections for at the specified measurement points are essentially similar: $\delta_{m1} \approx 0.43m$; $\delta_{m2} \approx 0.26m$; and $\delta_{m3} \approx 0.18m$. Thus implying that for $\phi_{av} < 50^o$ the transverse loads across the stack are independent of friction angle along joints. Most of the deformation is achieved trough inter-block shear since lateral thrust is not fully developed and the gravitational load is not equilibrated, leading to progressive failure.

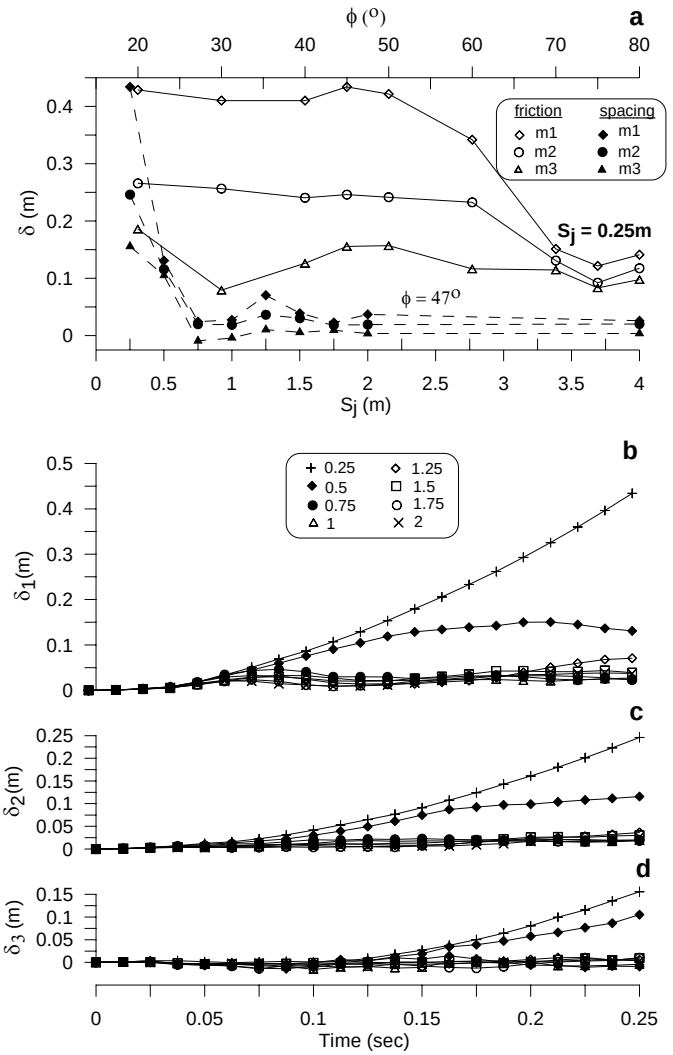

Figure 9. a) DDA prediction for mid-span deflection at the measurement points *m1, m2* and *m3* a) as friction angle (ϕ) and joint spacing (S_j); Time histories for different values of joint spacing for measurement points: b) *m1*; c) *m2*; d) *m3*

5.3 *Limitations of DDA analysis*

DDA analysis of the Tel Beer-Sheva water reservoir suffers from a number of drawbacks associated with geometrical definitions and numerical problems. These shortcomings affect DDA predictions when compared with findings at the site.

The dome like geometry of the failure area indicates that the problem is truly three dimensional (3-D) rather than two-dimensional (2-D). The stabilizing effect of the compressive stress in the normal to plane direction σ_{zz} is ignored. True 3-D modeling of the problem is extremely difficult, due to the ex-

tremely large number of block elements involved. For a single layer configuration the number of blocks is 1024, for sequence of layers configuration the number of blocks exceeds 10,000. The number of DDA deformation variables and degrees of freedom for 3-D DDA analysis is 3 and 12 respectively, compared with 2 and 6 for 2-D DDA analysis. The global stiffness matrix for a system of *n* blocks is *12n×12n* matrix. Thus, the global stiffness matrix becomes extensively large. Furthermore, contact formulation of the 3-D problem is difficult mainly due to great number of contacts involved and increased deformational freedom at each contact. The convergence of such a large system is extremely difficult and slow. At present, the applicability of 3-D DDA to full-scale problems is limited. Therefore, 2-D analysis is numerically and practically advantageous over 3-D analysis.

The fist order displacement approximation in DDA results in constant strain/stress elements, and stress concentrations within the blocks are not computed. The stability of the beams is however achieved trough rotation, which must produce stress concentration at the contact points. Therefore complete stress distribution for the entire domain region is not available. This shortcoming becomes with increase in block szia. Thus, for a system consisting of a large number of small blocks, as in the case of Tel Beer-Sheva, the stress distribution computed by DDA may be assumed sufficiently accurate.

6 COMPARISON BETWEEN DDA AND VOUSSOIR METHODS

From the described above it is concluded that classic Voussoir procedure (Evans, 1941; Beer and Meek 1982) is unconservative, predicting required friction angles for roof stability lower than the available friction angle along joints. The unconservative nature of the analysis can be attributed to the following factors: 1) Large number of discontinuities_- the rotational freedom required for stable arching in a multi-fractured beam is larger than the one required for a three-hinged beam; 2) Partial inter-bed separation - Voussoir analysis assumes that no gravitational load is transferred to the lower member of the beam stack. In the case of Tel Beer-Sheva this assumption is not satisfied, the failed rock mass consists of 4 individual beds. Thus, vertical load transfer between beams must be considered.

DDA analysis of a single layer with multiple joints showed that stability is assured for friction angles greater than 75^o. Clearly DDA prediction is more accurate than the Voussoir model, however conservative. DDA analysis showed that when the shear resistance along joints is increased stability is achieved trough increased rotation of blocks near the abutments. investigation of the block ratio effect showed that beam stability is improved for blocks with high aspect ratio, thus confirming the findings of Passaris et al., (1993).

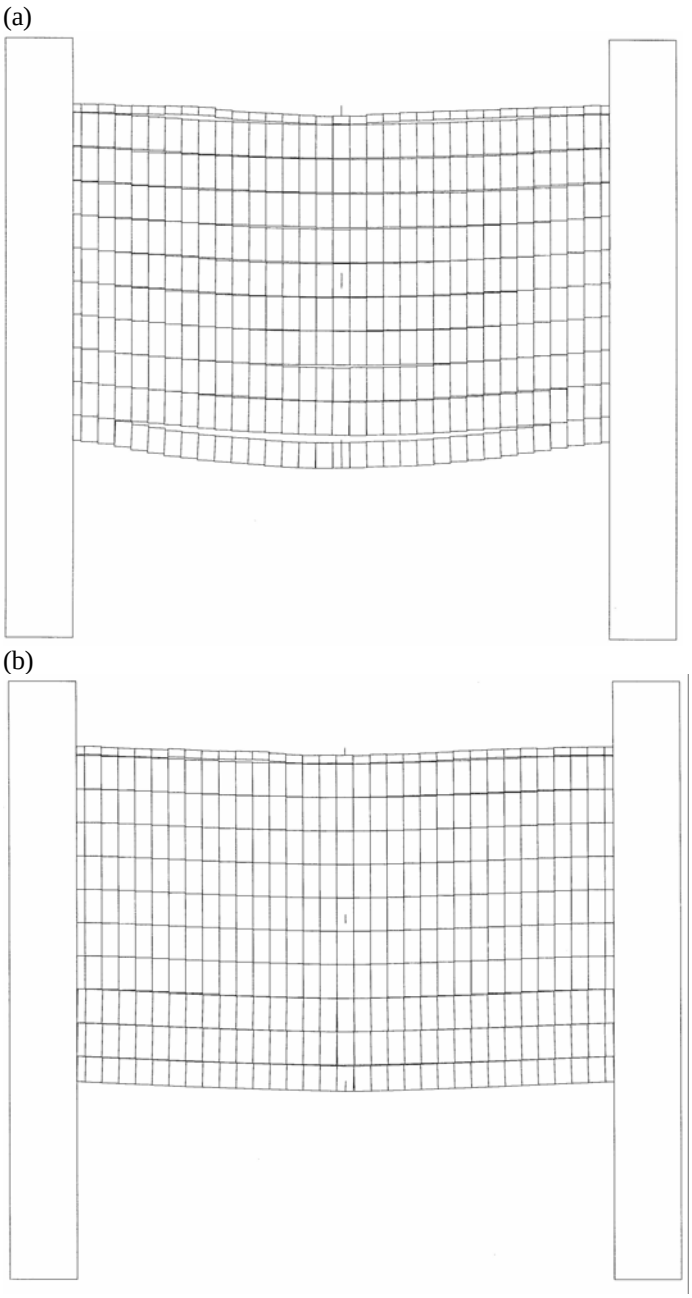

Figure 10. DDA graphic outputs of multi –layered roof deformation for $S = 8m$, $S_j = 0.25m$ and $t = 0.5m$ at $T = 0.25$ *sec*: a) $\phi = 50^o$; b) $\phi = 70^o$.

DDA analysis of a laminated Voussoir beam showed that for the case of Tel Beer-Sheva analysis of the immediate roof (i.e. single layer) is only partially applicable, given the fact that vertical load was transmitted vertically rather then laterally to the abutments. The stability of the laminated Voussoir is governed by similar processes: stability is achieved when shear resistance is sufficient to induce rotation of individual blocks close to the abutments. Then the global behavior of the layers is changed from a succession of layers each imposing vertical load on the layers bellow, to a coherent beam where loads are transformed latterly to the abutments. This transition is indicated by homogenization of deflection across the bulk of the sequence.

Development and Application of Discontinuous Modelling for Rock Engineering, Ming Lu (ed.) 2003 Swets & Zeitlinger, Lisse. pp: 93 – 102.

7 CONCLUSIONS

- Stability of a multi-jointed single layer is assured when the shear resistance along joints is sufficient to preclude inter-block shear, and to induce increased rotation near the abutments.
- Insufficient shear resistance along joints or high fracture density within a stack of layers results in: 1) transverse load transfer and 2) excessive differential displacements, which may lead to instability.
- Within a stack of layers, the transition from instability to stability is marked by reduction and homogenization of displacements.
- When compared with classic Voussoir model DDA analysis is found to be more accurate, conservative and realistic.

REFERNCES

Beer. G. and Meek, J.L. 1982. Design curves for roofs and hanging walls in bedded rock based on voussoir beam and plate solutions. *Trans. Inst. Min. Metal*. 91, A18-22.

Benary, R. 1996. *Stability of underground openings in jointed chalky rock – a case study from Tel Beer-Sheva*. M.Sc. Thesis. Department of Geol. and Env. Sci. Ben Gurion University.

Brady, B. H. and Brown, E. T. 1985. *Rock mechanics for underground mining. 1st ed.*, George Allen and Unwin, London. 527 pp.

Cundall, P. A. 1971. A computer model for simulating progressive, large scale movements in blocky rock system. *Symposium of International Society of Rock Mechanics*, Nancy, France. pp 11-18.

Diederichs, M. S. and Kaiser, P. K. 1999. Stability of large excavations in laminated hard rock masses: the voussoir analogue revisited. *Int. J. Rock. Mech.* 36: 97-117.

Doolin, D. and Sitar, N. 2002. Displacement accuracy of discontinuous deformation analysis method applied to sliding block. *Journal of engineering mechanics, ASCE*. 128 (11): 1158-1168.

Evans, W. H. 1941. The strength of undermined strata. *Trans. Inst. Min. Metal*. 50: 475-500.

Fayol, M. 1885. Sur les movements de terrain provoques par l'exploitation des mines. *Bull. Soc. Indust.* 14:818.

Goodman, R. E. 1989. *Introduction to rock mechanics. 2nd ed*. John Wiley & Sons. 562 pp.

Hatzor, Y. H. and Feintuch, A. (2001) The validity of dynamic block displacement prediction using DDA. *Int. J. of Rock Mech. and Min. Sci*. 38: 599 – 606.

Hatzor, Y. H. and Benary, R. 1998. The stability of a laminated voussoir beams: back analysis of a historic roof collapse using DDA. . *Int. J. Rock. Mech. Min, Sci.*. 35(2): 165-181.

ITASCA. 1993. *Universal Distinct Element Code – UDEC*.

Jing, L. and Hudson, J. A. 2002. Numerical methods in rock mechanics. *Int. J. Rock. Mech. Min, Sci.*. 39: 409-427.

MacLaulghlin, M. 1997. *Discontinuous Deformation Analysis of the kinematics of land slides*. Ph. D. Thesis, Department of Civil Engineering, University of California, Berkley.

McBride, A. and Scheele, F. (2001) Investigation of discontinuous deformation analysis using physical laboratory models. In: Bicanic, N. (ed.). *Proc. of the Fourth International Conference on Discontinuous Deformation Analysis*. 73-82.

Nomikos, P. P., Sofianos A. I. amd Tsoutrelis, C. E. 2002. Structural response of vertically multi-jointed roof rocl beams. *Int. J. Rock. Mech. Min, Sci.*. 39: 79-94.

O'Sullivan, C. and Bray, J. D. (2001) A comparative evaluation of two approaches to discrete element modeling to particulate media. In: Bicanic, N. (ed.). *Proceedings of the Fourth International Conference on Discontinuous Deformation Analysis*. 97-110.

Obert, L. and Duvall, W. I. 1976. Rock mechanics and the design of structures in rock. 1st ed. John Wiley. 650 pp.

Passaris, E. K. S., Ran, J. Q. and Mottahed, P. 1993. Stability of the jointed roof in stratified rock. Int. J. Rock. Mech. Min, Sci. Geomech. Abstr. 30(7): 857-860.

Ran, J. Q., Passaris, E. K. S. and Mottahed, P. 1994. Shear sliding failure of the jointed roof in laminated rock mass. Rock. Mech. Rock. Eng. 27(4): 235-251.

Shi, G-h. 1988. Discontinuous Deformation Analysis – a new numerical method for the stsics and dynamics of block system. Ph. D. Thesis, Department of Civil Engineering, University of California, Berkley. 378p.

Shi, G-h. 1993. Block System Modeling by Discontinuous Deformation Analysis. Topics in Engineering Vol. 11, Computational Mechanics Publications. 209p.

Sofianos, A. I. and Kapenis, A, P. 1998. Numerical evaluation of the response in bending of an underground hard rock voussoir beam roof. *Int. J. Rock. Mech.*. 35(8): 1071-1086.

Tsesarsky, M., Hatzor, Y.H. and Sitar, N. 2002. Dynamic block displacement prediction – validation of DDA using analytical solutions and shaking table experiments. In: Hatzor, Y.H. (ed). *Proceedings of the 5th International conference on analysis of discontinuous deformation*. 195-206

Wright, F. D. 1972. Arching action in craked roof beams. 5th Int. *Strata Control. Conf*. 29: 1-9.

Yeung, M. R. 1991. *Application of Shi's Discontinuous Deformation Analysis to the study of rock behavior*. Ph. D. Thesis, Department of Civil Engineering, University of California, Berkley. 341p.